Formation process of recent fumarolic gases at the Mt. Mihara summit peak of the Izu-Oshima volcano, Japan

Takeshi Ohba

Volcanic Fluid Research Center, Tokyo Institute of Technology, 2-12-1 Ookayama, Meguro, Tokyo 152-8551, Japan

We have investigated the chemical and isotopic composition of recently formed gases emitted by three fumaroles on the Mt. Mihara summit peak of the Izu-Oshima volcano in order to assess the formation process of these gases. The CO_2/H_2O ratio of these gases varied greatly, with the δD and $\delta^{18}O$ of the H_2O being as low as a vapor phase equilibrated with the local meteoric water. These features are explained by a mixing of the vapor equilibrated with local meteoric groundwater and primary steam, which is a vapor phase generated by the mixing of magmatic gas and a cold meteoric groundwater. We concluded that there was no direct mixing between the magmatic vapor and a vapor phase of meteoric origin in the processes involved in fumarolic gas formation.
Key words: Fumarolic gases, formation process, Izu-Oshima volcano, CO_2/H_2O ratio, δD and $\delta^{18}O$ values.

1. Introduction

Izu-Oshima is an insular volcano located in the Pacific Ocean (Fig. 1) which has shown intermittent eruptive activities. In 1986, a sequence of eruptions occurred, the magnitude of which was relatively large compared to those of previous eruptions (Fuji *et al.*, 1988; Kawanabe, 1998). The 1986 eruptions produced lava flows on the northern west flank of the volcano, near the residential area of the island, necessitating that all residents of the island (up to 10,000) be evacuated. It is therefore necessary to assess the danger posed by this volcano by monitoring its activity with the aim of predicting future eruptions and thereby mitigating its threat to the residents of the island.

In general, the flux of magmatic CO_2 is expected to increase prior to the eruption, if the eruption is due to the ascent of magma (Notsu *et al.*, 2006). Suwa and Tanaka (1959) found a pre-eruptive increase in the temperature of fumarolic gases at Mt. Mihara, which is the summit peak of the Izu-Oshima volcano. According to Shimoike and Notsu (2000), the CO_2 concentration in steam, which is discharged at the bore hole drilled on the northern flank of volcano, gradually decreased after the eruption in 1986, although there are annual fluctuations. The $^3He/^4He$ ratio in the steam started to increase immediately after the eruption in 1986, reaching a maximum in later in 1986, before it decreased gradually (Sano *et al.*, 1995). These observations suggest that the temperature of fumarolic gases and the chemical composition of volcanic fluid are intimately related to the activity of the Izu-Ohsima volcano.

Kazahaya *et al.* (1993) sampled and analyzed the fumarolic gases produced between 1988 and 1991 at Mt. Mihara. Their analyses of the hydrogen and oxygen isotopes

revealed that the fumarolic gases were a mixture of magmatic vapor, meteoric water, and sea water. In 1988, the magmatic vapor comprised 70% fumarolic gases; this decreased to 40% in 1989, assuming that the δD and $\delta^{18}O$ of magmatic water was -27 and $+5.3$‰, respectively. The isotope ratio and chemical composition of fumarolic gases has not been assessed since 1989. The aim of this study, therefore, was to sample recently produced fumarolic gases in order to estimate the process of gas discharge formation at Mt. Mihara.

2. Sampling and Analysis of Fumarolic Gases

Fumarolic gases were sampled between 2004 and 2007 at the three fumaroles, Kengamine (K), A, and X-15, located on Mt. Mihara (Fig. 2). The flux of gases was largest at Kengamine (K), where the plume visible at a distance of 2 km, and the smallest at fumarole A, where it was difficult to recognize the plume at a distance of 200 m. The discharge of gases at X-15 was more active than that at A. The outlet temperature of the gases at X-15 has been monitored by the Japan Meteorological Agency (JMA).

The temperature of all fumarolic gases was less than 80°C. As all of the gases contained air, which prevented the use of normal sampling methods for fumarolic gas, such as those of Ozawa (1968) and Giggenbach (1975), we used the apparatus shown in Fig. 3(a) for the chemical analysis. Fumarolic gases were first washed with 20 ml of 5M KOH solution contained in an impinger, which was warmed with hot water to prompt the absorption of CO_2 by the KOH solution. A similar sampling method was employed by Taran *et al.* (2001) to sample a gas contaminated with air at the Colima volcano. The end of the sampling train was aspirated by a calibrated 100-ml glass syringe. The accumulated volume of aspirated gas was recorded. A desiccant tube containing $CaCl_2$ powder was attached to the end of the impinger to capture the water vapor released from the KOH solution. The other end of the desiccant tube was attached to a glass
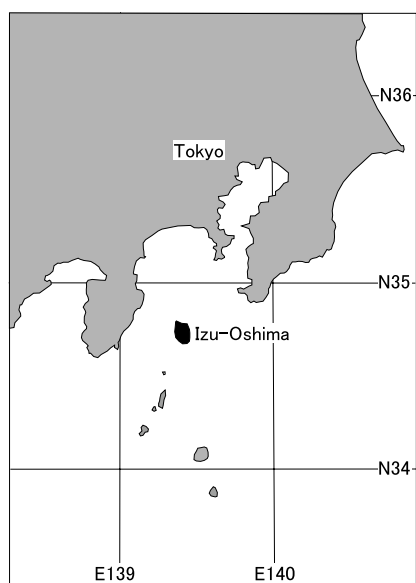
Fig. 1. The location of Izu-Oshima island.
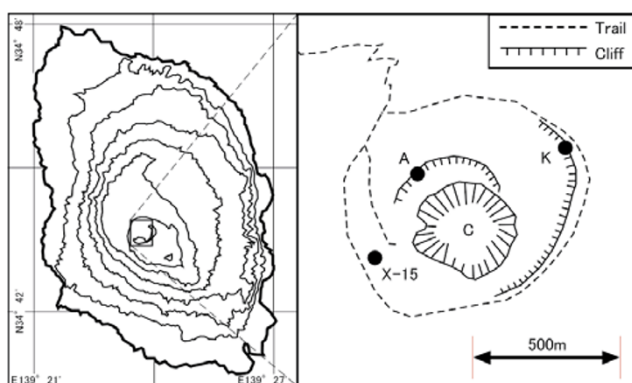
Fig. 2. *Left* Topography of the Izu-Oshima volcano with contours at 100-m intervals. *Right* The location of fumarolic gases emitted from fumaroles K, X-15, and A on Mt. Mihara.

tube with cocks to sample gases not absorbed by the KOH solution. There was no smell of H_2S and SO_2 at the fumaroles, and the absence of those gases was confirmed at the outlet of fumaroles by GASTEC detector tubes.

The sum of the weight of the impinger and the desiccant tube was determined before and after the sampling of the gas, and the weight increment was attributed to the sum of H_2O and CO_2 in the fumarolic gases. The air sampled in the glass tube was analyzed by a gas chromatograph with Ar carrier gas. The KOH solution in the impinger was made up to 100 ml with pure water. The amount of absorbed CO_2 in KOH was determined by micro-diffusion analysis (Conway, 1950). We did not analyze the sample for sulfur content because the absence of sulfur-bearing gases had been confirmed at the sampling site.

A condenser (Fig. 3(b)) was used to obtain the sample for the stable isotope analysis of H_2O vapor in fumarolic gas. A rolled rubber tube was immersed in water chilled with ice, and the fumarolic gas was passed through the tube. The condensed H_2O vapor was collected in a small glass bottle attached to one end of the chilled rubber tube. The collected
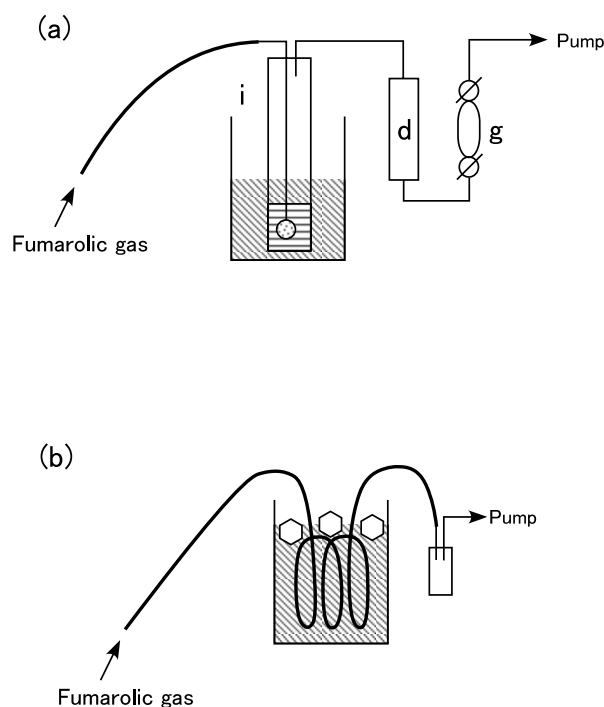
Fig. 3. Apparatus used for fumarolic gas sampling. The sampling trains in (a) and (b) were used for analyzing the chemical composition of gases and the stable isotopes, respectively. The i, d, and g in (a) is the impinger warmed with hot water, the desiccant tube, and the glass tube, respectively.

condensate was reduced to H_2 gas with metallic Zn (Coleman *et al.*, 1982). The H_2 gas so produced was subjected to stable isotope measurement on a MAT-252 mass spectrometer. The collected condensate was also equilibrated with CO_2 gas (Epstein and Mayeda, 1953) for the measurement of $\delta^{18}O$ on the MAT-252.

In order to measure $\delta^{13}C$ of CO_2 in the fumarolic gas, the gas was introduced into a 50-ml plastic syringe containing 10 ml of saturated $Ba(OH)_2$ solution. Once the fumarolic gas was in the syringe, a valve attached to the inlet of the syringe was closed, and the syringe was shaken vigorously to confirm the fixation of CO_2 gas as a $BaCO_3$ precipitate. The gas phase left in the syringe was discarded after shaking. The above procedure was repeated about 20 times to collect enough $BaCO_3$ precipitate for analysis. The collected precipitate of $BaCO_3$ was allowed to react with H_3PO_4 in vacuum to obtain pure CO_2 gas. The $\delta^{13}C$ of the prepared CO_2 gas was measured on the MAT-252.

3. Results

The outlet temperature, chemical composition, and isotope ratio of fumarolic gas are listed in Table 1. The collected fumarolic gas is a mixture of H_2O vapor, CO_2, H_2, and air. The outlet temperatures at K, X-15, and A were stable at 77–78, 65–66, and 57–58°C, respectively. The CO_2/H_2O ratio of gas at K was 0.0287–0.0297, which is much higher than that of the gas at X-15, which was 0.0063–0.00148. The CO_2/H_2O ratio of gas at A was 0.0147–0.0250, which is slightly lower than the ratio of gas at K. The isotope ratio of H_2O in the fumarolic gas at K and X-15 was −74 to −67‰ for δD and −12.5 to −10.8‰

Table 1. Chemical and isotopic composition of fumarolic gases at Izu-Oshima volcano.

Location	Date	Temp.	Gases excluding air				Air	H₂O		CO₂
			H_2O	CO_2	H_2	CO_2/H_2O		δD_{SMOW}	$\delta^{18}O_{SMOW}$	$\delta^{13}C_{PDB}$
		(°C)	mmol/mol	mmol/mol	mmol/mol	molar ratio	molar %	(‰)	(‰)	(‰)
K	2006/3/29	77.3	971.1	28.8	0.015	0.0297	52.9	−69	−11.0	−3.7
K	2007/4/2	78.5	972.1	27.9	0.0059	0.0287	55.4	−67	−10.8	−3.1
X-15	2004/3/9	65.0	991.3	8.7	na	0.0087	80.5	−71	−11.8	na
X-15	2005/11/16	66.5	993.7	6.3	na	0.0063	80.2	−74	−12.5	na
X-15	2006/3/29	66.2	985.4	14.6	0.0012	0.0148	83.2	−74	−11.8	na
X-15	2007/4/2	65.9	987.4	12.6	0.00054	0.0128	83.9	−72	−11.8	na
A	2004/3/10	56.0	975.6	24.4	na	0.0250	86.3	−91	−15.2	na
A	2005/11/16	57.4	985.6	14.4	na	0.0147	85.6	−91	−15.0	na

na: not analyzed

for $\delta^{18}O$. The δD and $\delta^{18}O$ values of H_2O at A were much lower than those at K and X-15. The $\delta^{13}C$ of CO_2 in the gas at K was −3.7 to −3.1‰, which is the value characteristic of H_2O of arc volcanic origin (Sano and Marty, 1995). The concentration of CO_2 in gas from X-15 and A was too low to collect enough $BaCO_3$ precipitate for isotope analysis. Although the level of H_2 in the gases from the three fumaroles varied greatly, the concentration of H_2 in the gas at K was almost tenfold higher than that in the gas at X-15.

4. Discussion
4.1 Condensation of water vapor

The correlation between the δD and $\delta^{18}O$ of H_2O in fumarolic gas is shown in Fig. 4, where the local meteoric water (MW) at the Izu-Ohsima volcano (Takahashi *et al.*, 2000), magmatic vapor (MV) characteristic of the subduction zone (Taran *et al.*, 1990; Giggenbach, 1992), and sea water (SW) are also plotted. The H_2O sampled by Kazahaya *et al.* (1993) in 1988–1991 plots within the triangle defined by MW, MV, and SW, suggesting that the H_2O was a mixture of those three end members. Izu-Oshima is an insular volcano. The section of the island lower than sea water level could be invaded by sea water. According to Kazahaya *et al.* (1993), cracks would have developed around the conduit beneath the crater after the eruption in 1986. Sea water could have been transported through these cracks to the conduit, resulting in the volcanic gas being contaminated with sea water. In December 1989, the isotope ratio of the fumarolic gas emitting from the fumaroles showed little contamination by sea water. This change was explained by Kazahaya *et al.* (1993) to be the result of crack closure.

The isotope ratio observed in this study was much lower than the H_2O reported by Kazahaya *et al.* (1993). Such a low isotope ratio might be explained by a partial condensation of H_2O vapor as condensation reduces the isotope ratios of the remaining H_2O vapor. This process is modeled by the Rayleigh fractionation process, expressed by,

$$\delta = (\delta_i + 1000)F^{\alpha-1} - 1000, \qquad (1)$$

where δ indicates the delta notation of D/H or $^{18}O/^{16}O$ of H_2O, subscript i indicates the state of the H_2O vapor prior to condensation, F indicates the fraction of H_2O vapor left after condensation, and α is the isotope fractionation factor between liquid water and vapor, the numerical value of which is listed in Table 2. The lines C1, C2, and C3 in
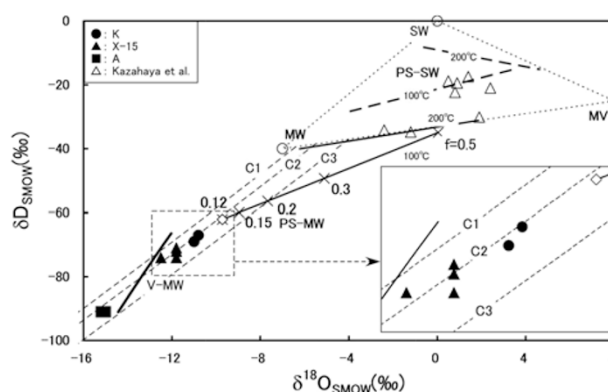
Fig. 4. Correlation between δD and $\delta^{18}O$ of H_2O in fumarolic gas with calculated primary steam and the end members producing the primary steam. The solid circle, solid triangle, and solid rectangle indicate the fumarolic gas at the K, X-15, and A, fumaroles, respectively. Open triangles indicate the fumarolic gas analyzed in 1988–1989 by Kazahaya *et al.* (1993). MV, MW, and SW are the magmatic vapor, local meteoric water, and sea water, respectively. The solid line denoted by PS–MW represents the primary steam at 100 and 200°C, allowing the freedom in the mixing fraction of MV. The dashed line denoted by PS–SW represents the primary steam at 100 and 200°C generated from the MV and SW. The solid line denoted by V–MW is a H_2O vapor equilibrated with MW at 50–100°C. The dotted lines denoted by C1, C2, and C3 indicate the trajectory of remained H_2O vapor left after the partial condensation of H_2O vapor. The starting stage of condensation was assumed to be located on the mixing line connecting MV and MW. The mixing fraction of MV in C1, C2, and C3 is 4, 10, and 20%, respectively. The diamond symbol indicates the potential end member of PS–MW to form fumarolic gases at K and X-15.

Fig. 4 indicate the change in the isotope ratio of the H_2O vapor where the fraction of condensation was allowed to be variable. The condensation was assumed to take place at 100°C. The isotope ratio of the H_2O vapor decreases during the process of condensation. The initial H_2O vapor before the start of condensation was assumed to be a mixture of MW and MV. Under the above assumption, C1, C2, and C3 comprise 4, 10, and 20% MV, respectively. The gases at K and X-15 are plotted along the line C2 (insert in Fig. 4).

The process of fumarolic gas formation could be analyzed more confidently by introducing the CO_2/H_2O ratio in the gas with the δD and $\delta^{18}O$ (Sawa *et al.*, 2006). In Fig. 5, the $\delta^{18}O$ of H_2O is correlated with the CO_2/H_2O ratio of the fumarolic gas. Because the concentration of carbonate and bicarbonate ions in MW and SW is low, even if MV

Table 2. Parameters used for the calculatioin on the composition of primary steam.

Term		Symbol	Value	Unit
Temperature of MV			1100	°C
Temperature of MW			18	°C
Enthalpy of MV		H_{MV}	4875	kJ/kg
Enthalpy of MW		H_{MW}	75	kJ/kg
Enthalpy of PS	at 100°C	H_{PS}	2677	kJ/kg
Enthalpy of PW	at 100°C	H_{PW}	417	kJ/kg
Enthalpy of PS	at 200°C	H_{PS}	2792	kJ/kg
Enthalpy of PW	at 200°C	H_{PW}	855	kJ/kg
δD of MV		δ_{MV}	-25	‰
δD of MW		δ_{MW}	-40	‰
δD of SW		δ_{SW}	0	‰
$\delta^{18}O$ of MV		δ_{MV}	8	‰
$\delta^{18}O$ of MW		δ_{MW}	-7	‰
$\delta^{18}O$ of SW		δ_{SW}	0	‰
CO_2/H_2O of MV		C_{MV}	0.04	
CO_2/H_2O of MW		C_{MW}	0	
CO_2/H_2O of SW		C_{SW}	0	
D/H fractionation factor	at 100°C	α	1.0283	
$^{18}O/^{16}O$ fractionation factor	at 100°C	α	1.00509	
CO_2/H_2O distribution coefficient	at 100°C	β	0.000215	
D/H fractionation factor	at 200°C	α	1.00237	
$^{18}O/^{16}O$ fractionation factor	at 200°C	α	1.00341	
CO_2/H_2O distribution coefficient	at 200°C	β	0.00266	

The value of α was given by Horita and Wesolowski (1994). The value of β was given by Giggenbach (1980). The value of enthalpy was referred to the standard steam table (e.g., Steam Table, Japan Society of Mechanical Engineers, Tokyo, 25 November 1999).

Table 3. Averaged CO_2/H_2O molar ratio of volcanic gases with high temperature.

Volcano				Temp	Reference
	Average	1σ	n	°C	
Colima	0.016	0.006	10	> 700	Taran *et al*. (2002)
Kudriavy	0.015	0.005	14	> 900	Korzhinnsky *et al*. (2002)
Momotombo	0.025	0.010	47	> 800	Menyailov *et al*. (1986)
Usu	0.018	0.009	18	> 600	Ossaka *et al*. (1984)
Unzen	0.020	0.007	7	> 700	Ohba *et al*. (1994)
Satsuma-Iwojima	0.0046	0.0012	8	> 700	Shinohara *et al*. (1993)

and SW were to be vaporized, the CO_2/H_2O ratio would be much lower than that of the MV. The CO_2/H_2O ratio in MW and SW was assumed to be zero in Fig. 5, while the CO_2/H_2O ratio of MV was assumed to be 0.04, so that the triangle regions defined by MV-MW-SW in Figs. 5 and 6 cover the points observed by Kazahaya *et al*. (1993). The CO_2/H_2O ratio of volcanic gas observed at several volcanoes is given in Table 3, where high-temperature gases were selected. Although the gas emitted by Satsuma Iwojima has an exceptionally low ratio, the ratio of the most of the volcanoes is restricted to less than 0.035. The assumed value for Izu-Oshima, 0.04, is close to the highest ratio observed at the volcanoes presented in Table 3.

Figure 5 shows the change in the CO_2/H_2O ratio and $\delta^{18}O$ of H_2O due to condensation. The change in the CO_2/H_2O ratio by condensation of H_2O vapor is expressed by,

$$C = C_i F^{\beta-1}, \qquad (2)$$

where C indicates the CO_2/H_2O ratio of fumarolic gas, and β indicates the CO_2/H_2O distribution factor between H_2O

liquid and vapor, the numerical value of which is shown in Table 2. The observed fumarolic gases in this study are distributed along the condensation curves C1, C2, and C3, which represent initial mixtures of 4, 10, and 20% magmatic vapor, respectively. Notice that the fumarolic gases emitted at the K fumarole plot along C3. A high CO_2/H_2O ratio requires the fraction of MV to be as high as 20%. In contrast, the low CO_2/H_2O ratio at the X-15 fumerole requires 4–10% of mixing with MV, a much lower mixing ratio relative to the fumarolic gas at K. The distribution of observed fumarolic gases in Fig. 5 is also similar to the distribution shown in Fig. 6 where the CO_2/H_2O ratio is correlated with δD. In Fig. 4, the contribution of MV is about 10% for the fumarolic gases emitted at both K and X-15.

In terms of the mixing ratio of MV, the interpretation based on the correlation in Fig. 4 is inconsistent with that in Figs. 5 and 6, suggesting that a simple mixing between MV and MW and a subsequent condensation of H_2O vapor can not explain the observed correlation among $\delta^{18}O$, δD, and the CO_2/H_2O ratio.
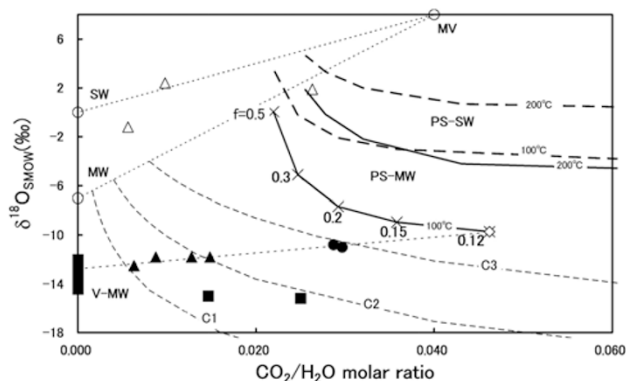
Fig. 5.   Correlation between the $\delta^{18}O$ of H_2O and the CO_2/H_2O ratio of fumarolic gas with calculated primary steam and the end members producing the primary steam. See Fig. 4 for the definition of the symbols. Three of the data points by Kazahaya *et al.* (1993) are given only because the other data were not accompanied by the CO_2/H_2O ratio.
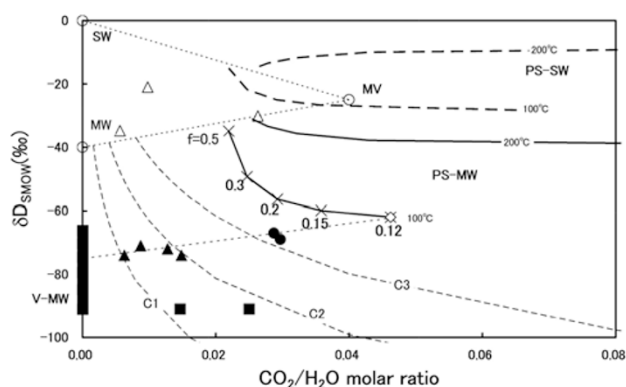
Fig. 6.   Correlation between the δD of H_2O and the CO_2/H_2O ratio of fumarolic gas with calculated primary steam and the end members producing the primary steam. See Fig. 4 for the definition of the symbols. Only three of the data points of Kazahaya *et al.* (1993) are given in the figure.

4.2   Primary steam

As described in the previous section, the correlation between the CO_2/H_2O ratio and stable isotope ratios can not be explained by direct mixing between MV and MW and a subsequent partial condensation of H_2O vapor. I propose an alternative explanation based on three facts/observations: (1) thermal water was discharged from a bore hole on the northern middle flank of Izu-Oshima volcano; (2) the steam discharged with this thermal water contains CO_2 gas of magmatic origin; (3) the concentration of CO_2 in the steam has been affected by the volcanic activity of Izu-Ohshima (Shimoike and Notsu, 2000). In addition, the thermal water discharged from active volcanoes has been explained by a mixing of magmatic fluid and groundwater of meteoric origin (Henley and Ellis, 1983), and the origin of the fumarolic gas has been explained by the formation of steam, which was created by the mixing of MV and meteoric groundwater, based on stable isotope ratio of H_2O (Giggenbach and Stewart, 1982). In this section, the observed fumarolic gas is modeled by the steam derived from MV and MW. A similar argument has been made by Taran *et al.* (1997) for the interpretation of boiling temperature fumarolic gas at Abacha volcano.

Following Giggenbach and Stewart (1982), the steam and the coexisting liquid generated by mixing between MV and MW is referred to as "Primary steam (PS)" and "Primary water (PW)", respectively. The CO_2/H_2O ratio and stable isotope ratio of PS can be estimated by solving the following equations.

$$H_{MV} f + H_{MW}(1 - f) = H_{PS} g + H_{PW}(1 - g) \qquad (3)$$

$$\delta_{MV} f + \delta_{MW}(1 - f) = \delta_{PS} g + \delta_{PW}(1 - g) \qquad (4)$$

$$C_{MV} f + C_{MW}(1 - f) = C_{PS} g + C_{PW}(1 - g) \qquad (5)$$

$$\alpha = \frac{\delta_{PW} + 1000}{\delta_{PS} + 1000} \qquad (6)$$

$$\beta = \frac{C_{PW}}{C_{PS}} \qquad (7)$$

In Eq. (3), H indicates the enthalpy of MV, MW, PS, and PW, and f and g indicate the mixing fractions of MV and generating fraction of PS, respectively. In general, g is not equal to f. Equations (3), (4) and (5) describe the conservation of enthalpy, isotope ratio, and CO_2/H_2O ratio (C), respectively, during the mixing of fluids and the separation to PS and PW. Equations (6) and (7) describe the equilibrium between PS and PW in terms of stable isotopic fractionation and CO_2 distribution. The numerical values used for calculating the CO_2/H_2O ratio and the stable isotope of PS are summarized in Table 2. Here I define PS–MW and PS–SW, which is the primary steam generated from the mixing of MV with MW and SW, respectively. The composition of PS–SW can be obtained in the same manner as that for PS–MW based on Eqs. (3)–(7), by substituting SW for MW.

Allowing freedom for the f value, the CO_2/H_2O and stable isotope ratios of PS are expressed as the solid and dashed curves in Figs. 5 and 6. As the temperature of PS and PW is unknown, two cases were considered where the temperature was 100 and 200°C, respectively. In Figs. 5 and 6, the CO_2/H_2O ratio of PS increases and the isotope ratio decreases as f decreases. At the left and right ends of the PS curve in Figs. 5 and 6, the f value is 0.5 and 0.12, respectively, at 100°C; at the left and right ends of the PS curve, the f value is 0.6 and 0.2, respectively, at 200°C.

According to Kazahaya *et al.* (1993), heated groundwater of a meteoric origin existed in the volcanic body of Mt. Mihara. Here, a vapor phase equilibrated with the meteoric water at 50–100°C is introduced as V–MW. The range of the V–MW is shown in Figs. 5 and 6 on the lower part of the y-axis. The observed fumarolic gases at K and X-15 are located between the V–MW and the right end of PS–MW curve at 100°C (diamond-shaped symbols). Therefore the high CO_2/H_2O ratio of the gas at K can be attributed to the large contribution of PS–MW at 100°C. In Fig. 3, PS–MW at 100°C is represented by a line. The isotope ratios of the observed fumarolic gases are plotted between the diamond symbol and V–MW. By introducing the PS, the correlation between the CO_2/H_2O ratio and the stable isotope ratio of H_2O can be explained consistently. In the above model, the condensation of H_2O vapor is not necessary to explain the composition of the gases at K and X-15. However, the low isotope ratio of gas at A requires a partial condensation
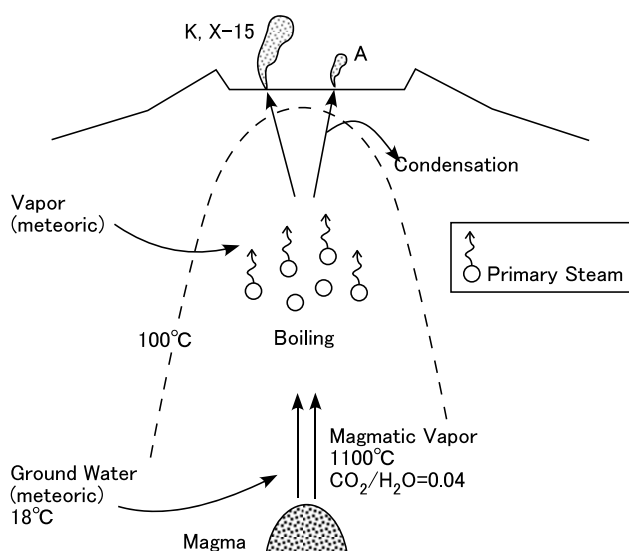
Fig. 7. Schematic view of the hydrothermal system generating the fumarolic gases. The dashed curve shows the isotherm of 100°C.

of H_2O vapor. Based on observations of the JMA, the outlet temperature of X-15 has been quite stable and has not shown any annual change. In the above model, the fumarolic gas at X-15 is a mixture of PS and V–MW. Both PS and V–MW would have a large heat capacity because they develop in a volcanic body. The stability of the outlet temperature at X-15 supports the above model for fumarolic gas formation.

The PS–MW at 200°C and PS–SW at both 100 and 200°C seems to be inappropriate for the end member of fumarolic gas because if those vapors are the end members, the mixing line connecting V–MW would have to have a steep positive slope in Figs. 5 and 6.

5. Conclusions

The formation of fumarolic gas is schematically described in Fig. 7. If we ignore the CO_2/H_2O ratio of the fumarolic gas, its formation might be explained by the direct mixing of MV and MW and a subsequent partial condensation of H_2O vapor, based on δD and $\delta^{18}O$ of H_2O. The observed CO_2/H_2O ratio in fumarolic gas has a large variation, which is difficult to explain based on the direct mixing of MV and MW.

The introduction of the primary steam component with a vapor phase originating in meteoric groundwater reproduces a gas phase whose isotope ratio is comparable to that of the observed fumarolic gas with variable CO_2/H_2O ratio. The interaction of magmatic fluid and meteoric groundwater and the subsequent formation of steam, as shown in this study, is one of the features common to volcanic hydrothermal systems (Henley and Ellis, 1983).

References

Coleman, M. L., T. J. Shepherd, J. J. Durham, J. E. Rouse, and G. R. Moore, Reduction of water with zinc for hydrogen isotope analysis, *Anal. Chem.*, **54**, 993–995, 1982.

Conway, E. J., *Microdiffusion analysis and volumetric error, 3rd edn.*, Crosby-Lockwood, London, 1950.

Epstein, S. and T. K. Mayeda, Variation of ^{18}O content of waters from natural sources, *Geochim. Cosmochim. Acta*, **4**, 213–224, 1953.

Fujii, T., S. Aramaki, T. Kaneko, K. Ozawa, Y. Kawanabe, and T. Fukuoka, Petrology of the lava and ejecta of the November, 1986 eruption of Izu-Oshima volcano, *Bull. Volcanol. Soc. Jpn.*, **33**, S234–S254, 1988 (in Japanese with English abstract).

Giggenbach, W. F., A simple method for the collection and analysis of volcanic samples, *Bull. Volcanol.*, **39**, 132–145, 1975.

Giggenbach, W. F., Geothermal gas equilibria, *Geochim. Cosmochim. Acta*, **44**, 2021–2032, 1980.

Giggenbach, W. F., Isotopic shifts in waters from geothermal and volcanic systems along convergent plate boundaries and their origin, *Earth Planet. Sci. Lett.*, **113**, 495–510, 1992.

Giggenbach, W. F. and M. K. Stewart, Processes controlling the isotopic composition of steam and water discharges from steam vents and steam-heated pools in geothermal areas, *Geothermics*, **11**, 71–80, 1982.

Henley, R. W. and A. J. Ellis, Geothermal systems ancient and modern: A geochemical review, *Earth Sci. Rev.*, **19**, 1–50, 1983.

Horita, J. and D. J. Wesolowski, Liquid-vapor fractionation of oxygen and hydrogen isotopes of water from the freezing to the critical temperature, *Geochim. Cosmochim. Acta*, **58**, 3425–3437, 1994.

Kawanabe, Y., Geological map of Izu-Oshima volcano. Geological map of volcanoes, Geological Survey of Japan, 1998.

Kazahaya, K., M. Takahashi, and A. Ueda, Discharge model of fumarolic gases during post-eruptive degassing of Izu-Oshima volcano, Japan, *Geochem. J.*, **27**, 261–270, 1993.

Korzhinsky, M. A., R. E. Botcharnikov, S. I. Tkachenko, and G. S. Steinberg, Decade-long study of degassing at Kudriavy volcano, Iturup, Kurile Islands (1990–1999): Gas temperature and composition variations, and occurrence of 1999 phreatic eruption, *Earth Planets Space*, **54**, 337–347, 2002.

Menyailov, I. A., L. P. Nikitina, V. N. Shapar, and V. P. Pilipenko, Temperature increase and chemical change of fumarolic gases at Momotombo volcano, Nicaragua, in 1982–1985: Are these indicators of a possible eruption?, *J. Geophys. Res.*, **91**, 12199–12214, 1986.

Notsu, K., T. Mori, S. C. DoVale, H. Kagi, and T. Ito, Monitoring quiescent volcanoes by diffuse CO_2 degassing: Case study of Mt. Fuji, Japan, *Pure Appl. Geophys.*, **163**, 825–835, 2006.

Ohba, T., J. Hirabayashi, and M. Yoshida, Equilibrium temperature and redox state of volcanic gas at Unzen volcano, Japan, *J. Volcanol. Geotherm. Res.*, **60**, 263–272, 1994.

Ossaka, J., J. Hirabayashi, and T. Ozawa, Chemical compositions of volcanic gases collected after the 1977 eruption of Usu volcano. Joint geophysical and geochemical observations: Usu volcano (September–December, 1982) and Tarumai volcano (September–October, 1983), 117–126, 1984 (in Japanese).

Ozawa, T., Chemical analysis of volcanic gases: I. Chemical analysis of volcanic gases containing water vapor, hydrogen chloride, sulfur dioxide, hydrogen sulfide, carbon dioxide, etc., *Geochem. Int.*, **5**, 939–947, 1968.

Sano, Y. and B. Marty, Origin of carbon in fumarolic gas from island arcs, *Chem. Geol.*, **119**, 265–274, 1995.

Sano, Y., T. Gamo, K. Notsu, and H. Wakita, Secular variations of carbon and helium isotopes at Izu-Oshima volcano, Japan, *J. Volcanol. Geotherm. Res.*, **64**, 83–94, 1995.

Sawa, T., T. Ohba, and J. Hirabayashi, The hydrothermal system beneath Ohwakudani on Hakone volcano, Japan: Traced by stable isotope ratio of H_2O, *J. Nucl. Sci. Technol.*, **43**, 468–473, 2006.

Shimoike, Y. and K. Notsu, Continuous chemical monitoring of volcanic gas in Izu-Oshima volcano, Japan, *J. Volcanol. Geotherm. Res.*, **101**, 211–221, 2000.

Shinohara, H., W. F. Giggenbach, K. Kazahaya, and J. W. Hedenquist, Geochemistry of volcanic gases and hot springs of Satsuma-Iwojima, Japan: Following Matsuo, *Geochem. J.*, **27**, 271–285, 1993.

Suwa, A. and Y. Tanaka, The changes in the temperautres of the fumaroles in the crater of Miharayama, Oshima, in connection with the activities of the volcano, *Bull. Volcanol. Soc. Japan*, **13**, 107–118, 1959.

Takahashi, M., K. Abe, T. Noda, K. Kazahaya, N. Ando, and T. Soya, Koshimizu thermal spring formed in the 1986 eruption of Izu Oshima

volcano, *J. Balneological Soc. Jpn.*, **49**, 176–185, 2000 (in Japanese with English abstract).

Taran, Y. A., B. G. Pokrovskiy, and Y. M. Dubik, Isotope composition and origin of water in andesite magma, *Trans. USSR Acad. Sci.*, **304**, 199–202, 1990.

Taran, Y., C. B. Connor, V. N. Shapar, A. A. Ovsyannikov, and A. A. Bilichenko, Fumarolic activity of Avachinsky and Koryaksky volcanoes, Kamchatka, from 1993 to 1994, *Bull. Volcanol.*, **58**, 441–448, 1997.

Taran, Y., A. Bernard, J. C. Gavilanes, E. Lunezheva, A. Cortes, and M. A. Armienta, Chemistry and mineralogy of high-temperature gas discharges from Colima volcano, Mexico. Implications for magmatic gas?atmosphere interaction, *J. Volcanol. Geotherm. Res.*, **108**, 245–264, 2001.

Taran, Y., J. C. Gavilanes, and A. Cortes, Chemical and isotopic composition of fumarolic gases and the SO_2 flux from Volcan de Colima, Mexico, between the 1994 and 1998 eruptions, *J. Volcanol. Geotherm. Res.*, **117**, 105–119, 2002.

T. Ohba (e-mail: ohba@ksvo.titech.ac.jp)